Eur. Phys. J. E (2015) **38**: 4
DOI 10.1140/epje/i2015-15004-9

THE EUROPEAN PHYSICAL JOURNAL E

Regular Article

pH-switchable structural evolution in aqueous surfactant-aromatic dibasic acid system

Linet Rose J.[1], B.V.R. Tata[2], V.K. Aswal[3], P.A. Hassan[4], Yeshayahu Talmon[5], and Lisa Sreejith[1,a]

[1] Department of Chemistry, NIT Calicut, Kerala 673601, India
[2] Condensed Matter Physics Division, IGCAR, Kalpakkam, Tamilnadu
[3] Solid State Physics Division, BARC, Mumbi 40008, India
[4] Chemistry Division, BARC, Mumbi 40008, India
[5] Department of Chemical Engineering, Technion-Israel Institute of Technology, Haifa, 3200003, Israel

Received 11 July 2014 and Received in final form 31 December 2014
Published online: 29 January 2015 –

Abstract. Structural transitions triggered by *p*H in an aqueous micellar system comprising of a cationic surfactant (cetylpyridinium chloride) and an aromatic dibasic acid (phthalic acid) was investigated. Reversible switching between liquid-like and gel-like states was exhibited by the system on adjusting the solution *p*H. Self-assembled structures, responsible for the changes in flow properties were identified using rheology, light scattering techniques and cryogenic Transmission Electron Microscopy (cryo-TEM). High-viscosity, shear-thinning behavior and Maxwell-type dynamic rheology shown by the system at certain *p*H values suggested the growth of spheroidal/short cylindrical micelles into long and entangled structures. Light scattering profiles also supported the notion of *p*H-induced microstructural transitions in the solution. Cryo-TEM images confirmed the presence of spheroidal/short cylindrical micelles in the low-viscosity sample whereas very long and entangled thread-like micelles in the peak viscosity sample. *p*H-dependent changes in the micellar binding ability of phthalic acid is proposed as the key factor regulating the morphological transformations and related flow properties of the system.

1 Introduction

Sensitivity of surfactant micelles to external stimuli has drawn considerable interest in the area of soft matter research, owing to the ease of designing switchable fluids. External stimuli, which trigger reversible fluidity changes in surfactant solutions, can be light, temperature, *p*H, salt or electric field [1–7]. Among these, *p*H is widely accepted as a facile and economic trigger for fabricating tunable fluids by tailoring the aggregation properties of surfactant micelles [8–11]. Thread-like micelles (TLMs) are one of the most fascinating morphologies resulting from amphiphilic self-aggregation. Entanglement of sufficiently long TLMs into a transient network can induce viscoelastic properties to the solution. The ability of entangled micelles to break and reform reversibly under shear enables their use in thickening and drag reducing applications [12–14]. Very high zero shear viscosity and non-Newtonian flow behaviour make TLMs distinctive from their spherical analogues. Spherical micellar solution generally possesses water-like viscosity and shear-independent Newtonian fluidity. Inter conversion between spherical and thread-like morphologies can be achieved by the wise choice of additives and stimuli.

Herein we report a systematic study of *p*H-stimulated structural progressions in aqueous cationic micellar system comprising of cetylpyridinium chloride (CPC) as the surfactant and phthalic acid (PhA) as the additive. The cationic surfactant CPC is an active antiseptic and emulsifying ingredient in many personal care products [15]. Phthalic acid with polar carboxylic groups on an aromatic ring can be considered as a strongly binding counter ion. Polar aromatic additives are well known for their ability to get adsorbed on to the palisade layer of cationic micelles and transforming them to rod-like or thread-like geometry [16,17]. Huang and co-workers have demonstrated the efficiency of potassium phthalic acid to promote structural growth of cetyltrimethylammonium bromide (CTAB) micelles into long and entangled structures in aqueous medium and proposed a facile route to design *p*H-switchable fluids, by making use of surfactant-hydrotrope interaction [10]. CPC is quite distinctive from CTAB, in terms of its head group, counter ion, hydrophobicity and micellization capabilities. As the head group size of the surfactant determines the packing of monomers, a different packing is expected in the case of CPC and

[a] e-mail: lisa@nitc.ac.in

CTAB. Also, with aromatic pyridinium salts, there would be delocalization of charge and less charge shielding compared to trimethyl ammonium salts. These factors will obviously influence the additive binding, growth pattern and overall viscosity of the system [18]. This motivated us to carry out a systematic study of the *p*H-dependent changes in CPC-phthalic acid system and to explore the microstructural features using light scattering techniques and cryo-TEM imaging. We observed that, without any *p*H modifications, higher concentrations of phthalic acid are capable of inducing high viscosity and viscoelasticity to CTAB solution. But such a dramatic viscosity growth was not observed in CPC-PhA solution even at equimolar concentration. Samples exhibited Newtonian flow behaviour in all mixing fractions, which suggested the presence of spherical or short cylindrical micelles in the system. The presence of charged and bulky pyridinium head groups restricts close packing and elongation of CPC micelles [19]. Also, the charge screening offered by PhA molecules to CPC micelles, at its native *p*H, is insufficient to bring enormous elongation of micelles. However, on increasing the solution *p*H, a perceptible increase in viscosity was observed. Around *p*H 3 the system exhibited Maxwell-type viscoelastic response, as expected for TLMs. Beyond this *p*H, the system reverted back to low viscosity Newtonian fluid as reported in the case of CTAB-potassium phthalic acid system. Thus a cyclic transition between spherical and long cylindrical morphologies can be assumed in CPC-PhA solution on moving within *p*H range of 1.8–5.5. By proper adjustment of solution *p*H, reversible switching between water-like and gel-like states (from very low *p*H to *p*H 3) or the other way round (from $p\text{H} \approx 3$ to higher values) can be achieved in the system.

The ability of polar additives to assist the formation of elongated structures in aqueous micellar solution depends on the extent of ionization and hydrophobicity. Aromatic acids with two distinct pK_a values can show different modes of micellar interaction at different *p*H values [10, 11]. This leads to *p*H-sensitive fluidity changes, since each micellar morphology is characterized by its own flow pattern. The flow behaviour of CPC-PhA system at different *p*H values was studied by both steady shear and dynamic rheology. Steady shear approach measures the sample response to a constant shear rate and helps to construct the flow curve of the material whereas a deeper analysis of the viscoelastic properties can be achieved by dynamic rheological measurements [20]. The dynamic rheological data obtained for CPC-PhA samples at around *p*H 3 resembled Maxwell-type stress relaxation shown by TLMs. Dynamic light scattering studies revealed a progressive increase in the apparent hydrodynamic diameter of micelles till *p*H 2.9. Thereafter a reduction in hydrodynamic diameter was observed. These observations are consistent with the *p*H-induced structural changes in the system. The results from small angle neutron scattering at different *p*H values also supported the notion of *p*H triggered morphological transitions in CPC-PhA system. Finally, the coexistence of spherical and cylindrical micelles in the low viscosity sample and the presence of long and entangled TLMs in the high-viscosity sample were confirmed by cryo-TEM imaging. Thus, this work provides strong experimental evidences for *p*H switchable structural evolutions in aqueous CPC-PhA micellar solution.

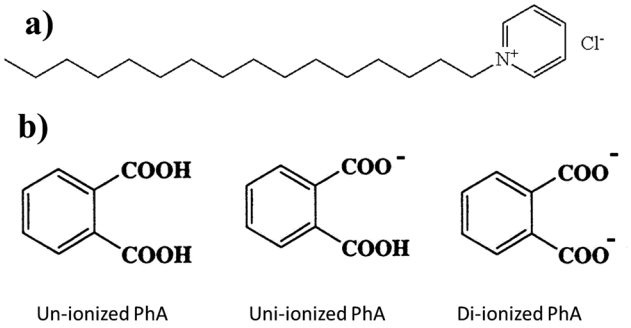

Fig. 1. Chemical structures of (a) cetylpyridinium chloride and (b) phthalic acid.

2 Materials and methods

2.1 Materials and sample preparation

CPC and phthalic Acid were purchased from BDH England (99% assay) and Sigma Aldrich (99.5% assay) respectively. All the chemicals were used as received. Samples were prepared in deionized Milli-Q water and kept in a water bath at 45 °C with stirring for about one hour for homogeneity. The resulting samples were stored at room temperature for at least one day before running experiments. *p*H of the solution was adjusted by adding micro volumes of aqueous solutions of NaOH or HCl (Nice Chemicals, India) and measured using Systronics digital *p*H meter-335 (±0.01). Figure 1 shows the chemical structures of CPC and PhA.

2.2 Rheological measurements

Rheological measurements were performed on an MCR-301 rheometer (Anton Paar, Germany) with a parallel plate measuring system (50 mm diameter). Sample temperature was maintained to the accuracy of ±0.01 °C. All the experiments reported below were conducted at a fixed temperature of 25 °C. The viscosities of samples were obtained from steady shear measurements with shear rate ranging from 0.001 to 100 s^{-1}. Dynamic frequency spectra were obtained in the linear viscoelastic regime of each sample as determined by strain sweep measurements. All the frequency sweep measurements were performed in the angular frequency range of 0.05–100 rad/s.

2.3 UV-vis spectroscopy

UV-visible spectra were recorded on a double beam spectrophotometer (Systronics, 2202) using quartz cuvette.

2.4 Fluorescence spectroscopy

Fluorescence spectra were obtained with LS 45 fluorescence spectrometer (PerkinElmer) using Nile Red as the fluorescence probe. 2.5 μM Nile Red was added to the surfactant solutions and stirred for 24 hours to reach equilibrium. The excitation wavelength of Nile Red was 575 nm and the fluorescence emission was monitored for surfactant solutions of different *p*H.

2.5 Dynamic Light Scattering (DLS)

DLS measurements were performed using Malvern 4800 Autosizer employing 7132 digital correlator (Malvern INstruments UK) at scattering angle of 130°. A vertically polarized light of wavelength 532 nm from a diode pumped solid state laser was used as the incident beam. The intensity correlation function was analyzed by the method of cumulants, where unimodal distribution of relaxation of time is considered.

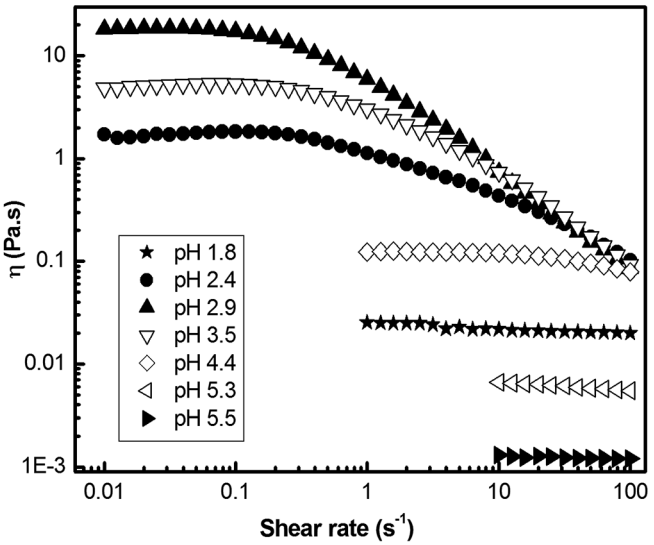

Fig. 2. Steady shear viscosity plot for 100 mM CPC/80 mM PhA solution at different *p*H values.

2.6 Small Angle Neutron Scattering

Neutron scattering experiments were carried out using SANS diffractometer at Dhruva Reactor, Bhabha Atomic Research Centre, Trombay. The mean wavelength of the incident neutrons is 5.2 Å and the angular distribution of the scattered neutrons were recorded using a one-dimensional position-sensitive detector. The diffractometer covers the scattering wave vector q range of 0.017–0.032 Å^{-1}. The sample was loaded in a quartz cell of 0.5 cm path length and the sample temperature was maintained at an accuracy of ±1 °C. The differential scattering cross section per unit volume, $I(q)$ of the sample was determined from the measured scattered neutron intensity as per the procedure described elsewhere [21].

2.7 Cryo-TEM

Vitrified cryo-TEM specimens were prepared in a controlled environment vitrification system (CEVS), at a controlled temperature and fixed relative humidity (100%). It is followed by quenching into liquid ethane at its freezing point. The specimens, kept below −178 °C, were examined by an FEI T12 G2 transmission electron microscope, operated at 120 kV, using a Gatan 626 cryo-holder system. Images were recorded digitally in the minimal electron dose mode by a Gatan US1000 high resolution cooled CCD camera with the digital micrograph software package.

3 Results and discussion

CPC is a well-known cationic surfactant capable of forming spherical micelles in aqueous medium. Certain strongly binding counter ions like sodium salicylate can aid the formation of long worm-like micelles in CPC solution [22,23]. We investigated the effect of phthalic acid, an aromatic dicarboxylic acid, on micellar growth in aqueous CPC system. The aqueous solubility of PhA is enhanced considerably in the presence of CPC, but no dramatic change in viscosity was observed visually. Though viscosity measurements revealed a slight viscosity increment on progressive addition of PhA to CPC solution, the solution remained water-like. Even 100 mM CPC/80 mM PhA solution showed a shear-independent Newtonian behaviour. But a dramatic change in viscosity was observed on gradually increasing the solution *p*H. Initially the water-like solution transformed to a viscoelastic fluid with gel-like appearance but, beyond certain *p*H values the water-like fluidity was re-established. The steady shear rheological response of 100 mM CPC/80 mM PhA solution at selected *p*H values is presented in fig. 2.

At *p*H 1.8 the solution was Newtonian with low viscosity, hinting the presence of spherical or short cylindrical micelles. On increasing the *p*H, zero shear viscosity showed an upward shift and a shear-thinning non-Newtonian flow pattern was observed around *p*H 3. Shear-thinning behaviour is typical of TLMs which can align under flow [24]. For the *p*H 2.9 sample, shear thinning started at lower shear rates. However with further increase in *p*H, zero shear viscosity decreased and the critical shear rate above which shear thinning begins shifted back to higher values. Shear-independent Newtonian flow pattern was observed again form *p*H 5.3 onwards.

Figure 3 shows the variation of zero shear viscosity with the solution *p*H. Viscosity reached a maximum at *p*H 2.9 and decreased thereafter. The initial viscosity growth along with the onset of shear-thinning behaviour suggests a structural modification of the small micelles to long and entangled worm-like micelles upon increasing the *p*H. A turnover in viscosity trend was observed beyond *p*H 2.9. Such peak behaviour in viscosity is widely reported in worm-like micellar literature and is

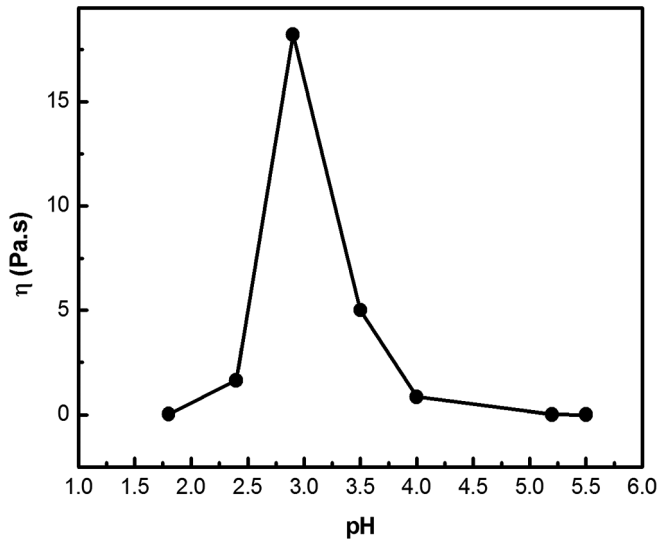

Fig. 3. Variation of zero shear viscosity *versus* *p*H for 100 mM CPC/80 mM PhA solution.

interpreted in terms of various phenomena such as micellar disintegration, branching or formation of bilayered structures [25–27].

The shear-thinning behaviour exhibited by the sample at certain *p*H values is a strong indication of existence of transiently networked structures in the system which can undergo reversible disruption under shear. The transient mesh resulting from the entanglement of elongated micelles can bring viscoelastic properties to the system.

Viscoelastic nature of micelle solution can be better inferred from the dynamic rheological measurements. TLMs are typical examples for Maxwell fluids with single relaxation time. The variation of elastic modulus (G') and viscous modulus (G'') with oscillatory shear frequency (ω) for Maxwellian fluids is given as

$$\boldsymbol{G'} = \frac{\omega^2\tau_R^2}{1+\omega^2\tau_R^2}\boldsymbol{G}_0, \tag{1}$$

$$\boldsymbol{G''} = \frac{\omega\tau_R}{1+\omega^2\tau_R^2}\boldsymbol{G}_0, \tag{2}$$

where G_0 is the plateau modulus (steady value of G' at high frequency) and τ_R is the relaxation time [28].The response of 100 mM CPC/80 mM PhA solution under oscillatory shear at different *p*H values are presented in fig. 4.

Maxwell-type behaviour, exhibiting a viscous nature at low ω and an elastic nature at high ω with a plateau for G' and minimum for G'', was closely followed at *p*H 2.9. Deviation from Maxwell behaviour was observed at high frequency. Such a deviation from the Maxwell pattern is predicted for worm-like micelles in terms of the Rouse mode relaxation at high frequency regime as shown by Granek and Cates [29]. In the low-frequency region the relaxation mechanism is governed by reptation and scission mode which strictly follows the Maxwell pattern [30]. At other *p*H values shown here, the sample exhibited a large deviation from Maxwell behaviour over the entire frequency range. Sample response showed a shift in the crossover frequency (ω_c, frequency at which G' and G'' cross) to higher-frequency region above *p*H 2.9. This signifies a reduction in relaxation time ($\tau_R = 1/\omega_c$) which in turn hints a shortening of micellar length beyond *p*H 2.9. Agreement to Maxwell model can be further confirmed by semi-circular shape of Cole-Cole plot (plot of G'' as a function of G'). The semicircle nature can be expressed as [31]

$$G''^2 + \left(G' - \frac{G_0}{2}\right)^2 = \left(\frac{G_0}{2}\right)^2. \tag{3}$$

The Cole-Cole plots for 100 mM CPC/80 mM PhA solution at different *p*H values are given in fig. 5.

The sample closely followed a semi-circular pattern at *p*H 2.9, but deviated considerably at other *p*H values shown in the plot. Oscillatory shear response of the samples together with the high viscosity observed in the steady shear rheology suggests the existence of entangled worm-like micelles in the system at and around *p*H 2.9. The departure from Maxwell behaviour, sequential reduction in relaxation time and the over turn in viscosity trend beyond *p*H 2.9 intimate shortening of the micellar length on further *p*H increment, eventually leading to the re-establishment of water-like state similar to the original solution (100 mM CPC/80 mM PhA solution without any *p*H modification).

UV-vis measurements were performed to investigate the changes in spectral pattern upon increasing the *p*H.

As shown in fig. 6, aqueous phthalic acid solution showed an absorbance maximum at 281 nm. This peak was retraced by the CPC–phthalic acid solution in its native *p*H, along with an additional peak at 258 nm with a shoulder, which corresponds to the UV absorption by CPC. A change in the absorbance pattern can be clearly noted in the spectrum obtained for CPC/PhA solution with *p*H > 5.5, which is in agreement with the formation of disodium phthalic acid at higher *p*H [10]. Thus the transformation of phthalic acid to di-ionised form in solution with *p*H above its second pK_a (5.43) can be inferred from the changes in the UV absorption behaviour.

Dynamic light scattering measurement was performed to get an insight of change in apparent hydrodynamic diameter of the aggregated structures with specific changes in *p*H. The intensity-weighed distribution of apparent hydrodynamic diameter is presented in fig. 7.

Up to *p*H 2.9, a successive shift towards a larger diameter region can be observed. This suggests an anisotropic growth of micelles to rod-like or to thread-like structures [19]. However, a backward shift towards the lower diameter region occurred on further increasing the *p*H to 5.5 which indicates shortening of micelles. DLS profile recommends that the *p*H-dependent changes in flow behaviour can be ascribed to the morphological transition between short and elongated micelles.

In order to further identify the microstructural features responsible for the *p*H-induced rheological changes, SANS analysis was performed on 100 mM CPC/80 mM PhA solution. Samples were made in D_2O to get the required contrast between micellar structures and solvent.

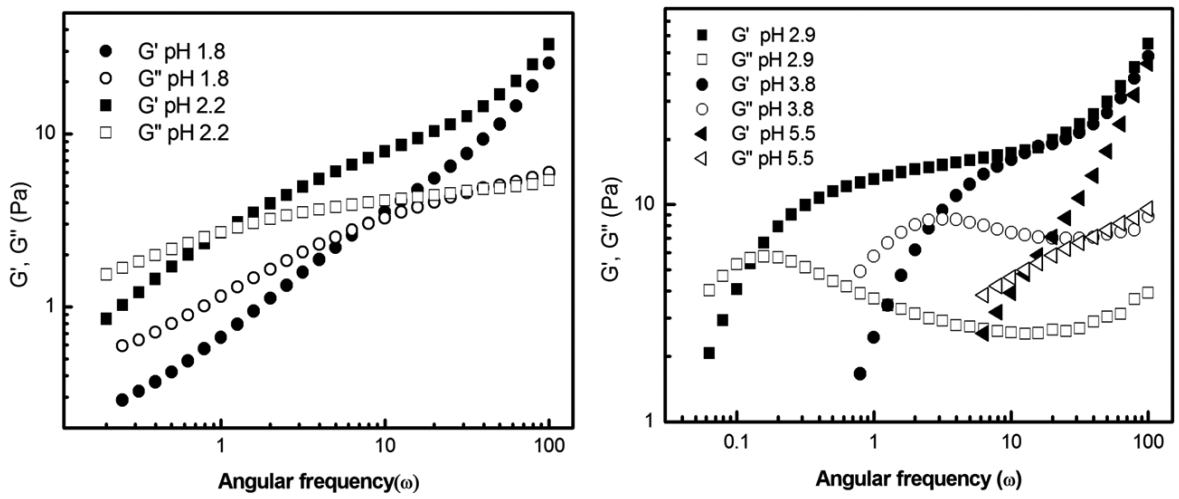

Fig. 4. Frequency spectrum of 100 mM CPC/80 mM PhA system at different *p*H values.

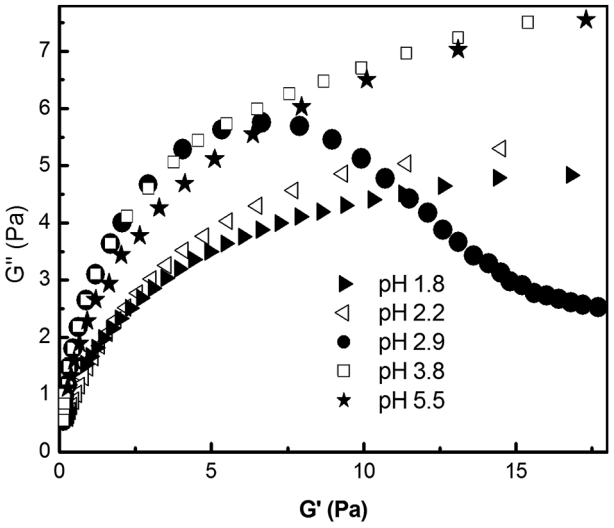

Fig. 5. Cole-Cole plot for 100 mM CPC/80 mM PhA solution at different *p*H values.

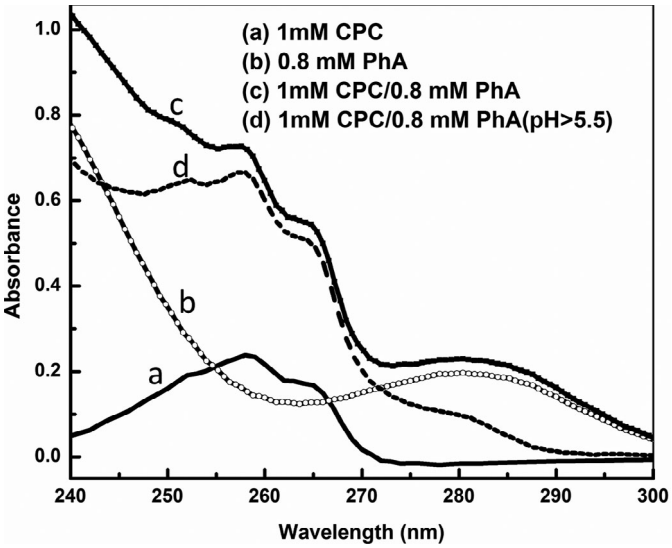

Fig. 6. UV–vis spectra of dilute solution of phthalic acid in the presence and absence of CPC.

SANS spectra obtained at three different *p*H values are shown in fig. 8.

The scattering profile at *p*H 1.8 showed a broad correlation peak in the low q region (at $q \sim 0.05\,\text{Å}^{-1}$) which is an indication of repulsive interaction between charged micellar heads. The peak appeared at $q_m \sim 2\pi/d$, where d is the average distance between micelles and q_m is the value of q at the peak position [32]. Significant rise in the scattering intensity and disappearance of correlation peak was seen at *p*H 2.9, implying an increase in the micellar dimension and decrease of effective charge per micelle. These observations along with the q^{-1} dependence as shown in fig. 8 strongly suggest scattering from elongated micelles at *p*H 2.9 [33]. Multiplication model, used to fit the experimental values appears to be in good agreement with the data (solid lines in fig. 8). The value of semi-minor axis obtained from large q data analysis of the SANS spectrum at *p*H 2.9 ($b \approx 20\,\text{Å}$) is comparable with the length of hydrocarbon chain of CPC molecule [19]. A considerably high value of semi-major axis ($a \approx 100\,\text{Å}$) hints at the one-dimensional elongation of micelles. However a reduction in scattering intensity and a plateau at low q region was observed in the SANS curve of the sample at a higher *p*H of 4.8 which suggests the presence of smaller micelles. The micelle radii obtained at this *p*H value with the aid of ellipsoid model fitting ($b \approx 19\,\text{Å}$ and $a \approx 30\,\text{Å}$) indicates a reduction in the micellar length and the existence of short rods or spherical micelles in the system. It can be seen from fig. 8 that the SANS data at high q region remains unaffected by *p*H changes, indicating a constant diameter for the micelles. The results obtained from SANS analysis are in good agreement with the rheology data, confirming *p*H-triggered structural evolutions capable of modifying the flow properties of 100 mM CPC/80 mM PhA solution dramatically.

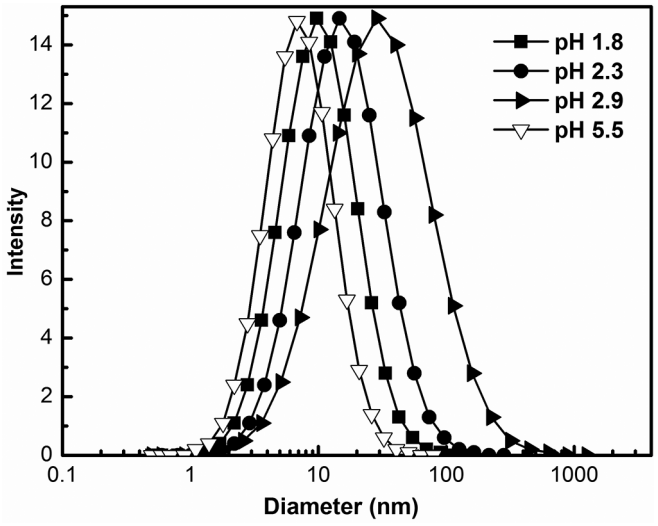

Fig. 7. Intensity-weighed distribution of apparent hydrodyanamic diameter of aggregates in 100 mM CPC/80 mM phthalic acid solution at different *p*H values.

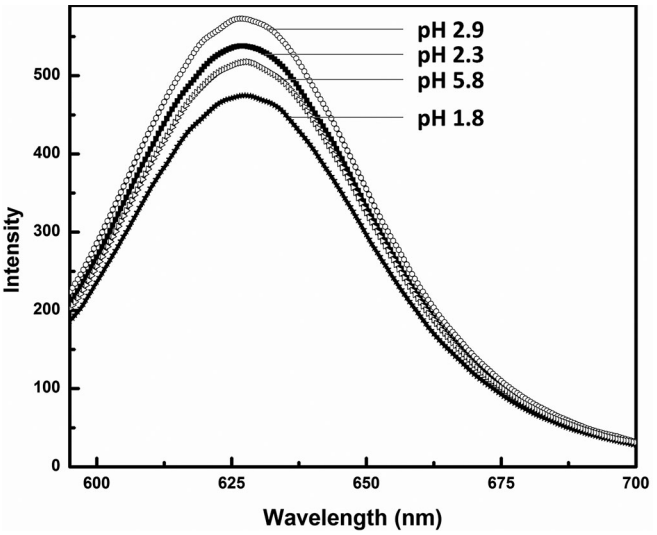

Fig. 9. Fluorescence emission spectra of Nile Red (2.5 μM) in 100 mM CPC/80 mM PhA solution at different *p*H values.

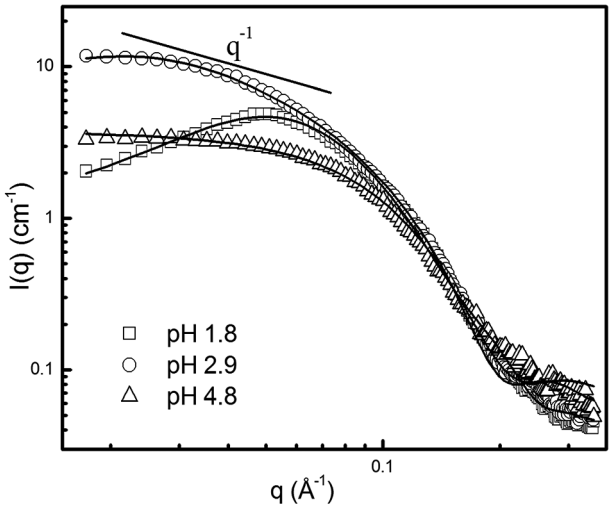

Fig. 8. SANS profile for 100 mM CPC/80 mM PhA solutions with varying *p*H at 40 °C. Solid lines represent fit to the data using models described in the text.

The alterations in the surfactant packing upon *p*H modification are reflected by the vertical shifts in fluorescence intensity of Nile Red incorporated into the micellar aggregates (fig. 9).

There was a perceptible increase in fluorescence intensity with increase in *p*H. Nile Red is a lipophilic dye, the fluorescence intensity of which varies depending on the hydrophobicity of the environment [34]. Noticeable increase in Nile Red fluorescence intensity in the CPC/PhA solution with successive increase in *p*H suggests that there is an expansion in the hydrophobic core volume of the micelles into which the stain is encapsulated. Elongated micelles are characterised by higher packing parameter ($p = v/a_0 l$, where v is the volume of hydrocarbon tail with a maximum effective length l and a_0 is the cross sectional area of the head group at the interface) as compared to spherical micelles [35]. The high p value of TLMs signifies increased volume of the hydrophobic micellar core. But beyond *p*H 2.9 a reduction in fluorescence intensity is observed indicating the shortening or disintegration of long micelles leading to shrinkage of hydrophobic core volume.

Transmission electron microscopy under cryogenic conditions is the most desirable technique for the direct visualisation of micellar morphology [36]. So in order to confirm unambiguously the structural transition responsible for the switching between water-like and gel-like state, we carried out the cryo-TEM imaging of 100 mM CPC/80 mM PhA solution at *p*H 1.8 and *p*H 2.9. The images are presented in fig. 10.

In fig. 10a, for the sample with unmodified *p*H (≈ 1.8), coexistence of spheroidal and short cylindrical/thread-like structures can be seen. From the steady shear rheology of the sample at *p*H 1.8, it can be assumed that micelles are not sufficiently long to induce viscoelasticity. The zero shear viscosity of the sample at *p*H 1.8 (≈ 0.001 Pa s) is similar to that of purely spherical micellar solution. But the cryo-TEM image of the sample revels that the system is not fully devoid of thread-like structures. Shikata *et al.* proposed that free counter ions in the bulk phase can catalyse entanglement scission of long micelles, thereby quickening the relaxation process and imparting high fluidity to the solution [37,38]. Since the selected concentration of additive is comparatively high and the extent of ionisation is weak, a larger fraction of unbound PhA molecules in the bulk phase could also contribute towards the water-like viscosity of the sample at low *p*H. Very long and entangled micelles responsible for the high viscosity and viscoelasticity of sample can be clearly seen at *p*H 2.9 (fig. 10b). Dark spots seen along with the entangled structures could be micellar end caps. Cryo-TEM images along with the Maxwell-type rheology strongly confirm that the viscoelasticity exhibited by the sample around *p*H 3 is due to the presence of highly entangled TLMs.

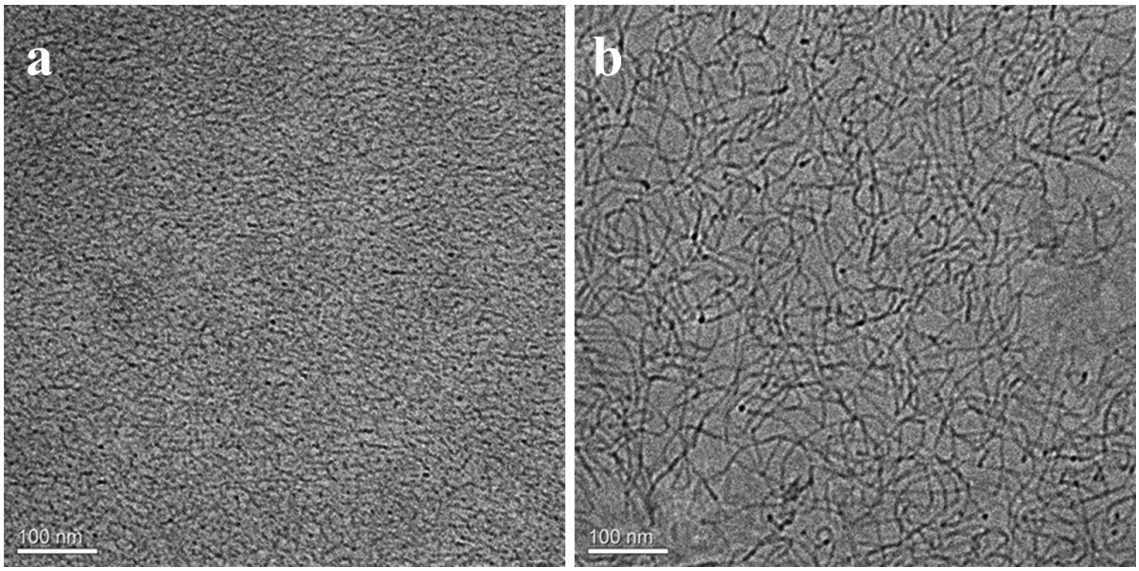

Fig. 10. Cryo-TEM images of 100 mM CPC/ 80 mM PhA sample at (a) *p*H 1.8 and (b) *p*H 2.9 (scale bar: 100 nm).

With the support of rheology, UV spectroscopy, fluorescence studies, DLS, SANS and cryo-TEM, the *p*H-sensitive rheological evolutions in the present micellar system can be ascribed to the cyclic structural transition between globular or short TLMs and highly entangled TLMs. The inability of PhA to bring viscoelasticity to CPC solution without the aid of *p*H modifications is obvious from the low-viscosity and Newtonian flow behaviour of the 100 mM CPC/80 mM sample at *p*H 1.8. Phthalic acid is an aromatic dicaroxylic acid with two distinct pK_a values, 2.94 and 5.43, respectively [39]. Solution *p*H can significantly influence the extent of ionization of PhA. 100 mM CPC/80 mM phthalic acid solution possesses a native *p*H of 1.8. At this *p*H, phthalic acid is weakly ionised and lesser extent of micellar binding is expected. On increasing the *p*H by adding NaOH, ionisation of PhA occurs to a larger extent. At *p*H close to the first pK_a of phthalic acid (2.94), the major structure will be sodium phthalic acid. With an aromatic ring bearing ionised carboxylic moiety, sodium phthalic acid can act as a strongly binding counter ion, which can effectively screen the head group charge thereby promoting enormous elongation of micelles. Under this circumstance, most of the hydrotrope ions will be in the micelle-bound state and fewer ions are available for catalysing entanglement scission. So the stress relaxation in the system is relatively slow, leading to very high viscosity and Maxwellian viscoelasticity. There are strong evidences for the formation of TLMs in aqueous micellar system comprising cationic surfactants and strongly binding aromatic counter ions [40,41,25]. Both the cryo-TEM image and SANS data support the existence of TLMs in the system around *p*H 3. With further increase in *p*H, sodium phthalic acid might transforms into disodium phthalic acid, as the solution approaches second pK_a of PhA, which is 5.43. Presence of two ionised carboxylic acid moieties modifies the hydrophilicity of phthalic acid resulting in increased solubility of disodium phthalic acid in water. The preference of disodium phthalic acid for aqueous medium reduces its binding to micelle surface resulting in the desorption of bound counter ions to water phase. The successive reduction in relaxation time and viscosity is a strong indication of progressive leaching out of phthalic acid molecules from the micelle surface on gradually increasing the *p*H to 5.5. This results in the shortening of micelles and recurring of water-like flow behaviour. Increased availability of free counter ions in the bulk water phase also contribute towards making the system more flexible. The structural transitions in micellar solution resulting from non-covalent counter ion binding can be controlled reversibly. The responsiveness of present micellar solution to *p*H favours its application as tunable fluid. The *p*H range within which gel-like to water-like transition takes place in CPC–PhA system (*p*H 2.9-5.5) was found to be similar to that reported for CTAB-potassium phthalic acid system, as it is dependent mainly on the pK_a values and binding ability of the dibasic acid used.

In order to make a comparison, we studied the effect of two other dicarboxylic acids, namely maleic acid and terephthalic acid on the *p*H-dependent viscosity behaviour of 100 mM CPC solution. Both the acids showed a negligible effect on the viscosity of aqueous CPC micelles. Maleic acid (MA), a non-aromatic dicarboxylic acid with pK_a values 1.92 and 6.23 [39] is fairly soluble in water. 100 mM CPC/80 mM MA solution showed water-like viscosity over the entire *p*H range monitored, which hints at the inability of MA molecules to offer effective charge screening to CPC micelles. Due to better aqueous solubility, MA molecules preferably remain in the medium than associating on to the CPC micelles. Increasing the *p*H of the solution merely improves the dissociation of acid molecules without altering the viscosity the system considerably. Unlike PhA, an aromatic ring capable of inducing hydrophobicity and promoting micellar binding is

absent in MA which could be the credible reason for the insensitivity of 100 mM CPC/80 mM MA micellar solution to *p*H changes. Terephthalic acid (tPhA) is isomeric with PhA. In PhA, the carboxylic acid groups are on adjacent positions whereas in tPhA they are para to each other. The geometrical features offer negligible dipole moment to tPhA and its water solubility in the absence of any alkali is much less. So we selected a lower concentration of tPhA (100 mM CPC/5 mM tPhA) for viscosity studies. Apart from improving the water solubility of tPhA, the increase of *p*H does not affect the viscosity trend of the solution. Even though tPhA possesses an aromatic ring to induce sufficient hydrophobicity, the structural trait of the molecule hinders its proper binding to CPC micelles even at high *p*H. The para-positioned functional groups remain as a barrier for the aromatic ring to bind to the micellar interface [42]. On the other hand, in PhA, the geometry highly favours its micellar binding.

The insignificant effect of MA and terephthalic acid on the *p*H-dependent viscosity behaviour of CPC solution reveals that both the optimum hydrophobicity and favourable geometry of PhA compliment the *p*H-sensitive structural changes in CPC/PhA micellar solution.

4 Conclusion

*p*H-responsive changes in the aggregation behaviour of CPC/phthalic acid micellar system in aqueous medium are demonstrated. System showed a cyclic transition between water-like and gel-like states within the *p*H range 1.8–5.5. Variations in molecular interactions between the surfactant and dicarboxlic acid at different *p*H values are considered as the key reason for structural and rheological modifications. Rheological results are in agreement with the proposed structural transitions in the system. Formation of elongated micelles at selected *p*H values and their disintegration upon further increase of *p*H were confirmed through SANS analysis. The presence of entangled TLMs responsible for the strong viscoelasticity of sample around *p*H 3 was further confirmed by Cryo-TEM imaging. The system can serve as a stmuli-responsive fluid with reversible control over viscosity.

This work was performed under the collaborative research scheme (CRS-K-0/5/20) of the UGC-DAE Consortium for Scientific Research, Kalpakkam node, India. The support and encouragement of Dr. G. Amarendra (scientist-in-charge, Kalpakkam node) is gratefully acknowledged. The cryo-TEM work was performed at the Laboratory for cryo-EM of Soft Matter, supported by the Technion Russell Berrie Nanotechnology Institute (RBNI). Authors are thankful to Dr. Ellina Kesselman and Dr. Judith Schmidt (Technion-Israel Institute of Technology) for their immense help in the cryo-TEM analysis. Thanks are due to Dr. K. Saravanakumar (IGCAR, Kalpkkam) for his help in carrying out the rheological experiments and Dr. C. Lakshmi (NIT, Calicut) for providing the fluorescence spectroscopy facility.

References

1. H. Sakai, Y. Orihara, H. Kodashima, A. Matsumura, T. Ohkubo, K. Tsuchiya, M. Abe, J. Am. Chem. Soc. **127**, 13454 (2005).
2. A.M. Ketner, R. Kumar, T.S. Davies, P.W. Elder, S.R. Raghavan, J. Am. Chem. Soc. **129**, 1553 (2007).
3. T.S. Davies, A.M. Ketner, S.R. Raghavan, J. Am. Chem. Soc. **128**, 6669 (2006).
4. H. Maeda, A. Yamamoto, M. Souda, H. Kawasaki, K.S. Hossain, N. Nemoto, M. Almgren, J. Phys. Chem. B **105**, 5411 (2001).
5. H. Kawasaki, M. Souda, S. Tanaka, N. Nemoto, G. Karlsson, M. Almgren, H. Maeda, J. Phys. Chem. B **106**, 1524 (2002).
6. S. Kumar, A.Z. Naqvi, Kabir-ud-Din, Langmuir **16**, 5252 (2000).
7. K. Tsuchiya, Y. Orihara, Y. Kondo, N. Yoshino, T. Ohkubo, H. Sakai, M. Abe, J. Am. Chem. Soc. **126**, 12282 (2004).
8. Y. Zhang, Y. Han, Z. Chu, S. He, J. Zhang, Y. Feng, J. Colloid Interface Sci. **394**, 319 (2013).
9. G. Verma, V.K. Aswal, P. Hassan, Soft Matter **5**, 2919 (2009).
10. Y. Lin, X. Han, J. Huang, H. Fu, C. Yu, J. Colloid Interface Sci. **330**, 449 (2009).
11. Z. Chu, Y. Feng, Chem. Commun. **46**, 9028 (2010).
12. J.F. Berret, *Rheology of wormlike micelles: Equilibrium properties and shear banding transitions*, in *Molecular Gels: Materials with Self-Assembled Fibrilles Networks*, edited by Richard G. Weiss, P. Terech (Springer, The Netherlands, 2006).
13. J. Yang, Curr. Opin. Colloid Interface Sci. **7**, 276 (2002).
14. H. Shi, Y. Wang, B. Fang, Y. Talmon, W. Ge, S.R. Raghavan, J.L. Zakin, Langmuir **27**, 5806 (2011).
15. S. Jenkins, M. Addy, R.G. Newcombe, J. Clin. Periodontol. **21**, 441 (1994).
16. V. Hartmann, R. Cressely, Colloid Surf. A **121**, 151 (1997).
17. H. Hoffmann, *Structure and Flow in Surfactant Solutions* (ACS, USA, 1994).
18. Kabir-ud-din, D. Bansal, S. Kumar, Langmuir **13**, 5071 (1997).
19. L. Abezgauz, K. Kuperkar, P.A. Hassan, O. Ramon, P. Bahadur, D. Danino, J. Colloid Interface Sci. **342**, 83 (2010).
20. M.E. Cates, S.J. Candau, J. Phys.: Condens. Matter **2**, 6869 (1990).
21. V.K. Aswal, P.S. Goyal, Curr. Sci. **79**, 947 (2000).
22. T. Mukhim, J. Dey, S. Das, K. Ismail, J. Colloid Interface Sci. **350**, 511 (2010).
23. J.F. Berret, Langmuir **13**, 2227 (1997).
24. D.P. Acharya, D. Varade, K. Aramaki, J. Colloid Interface Sci. **315**, 330 (2007).
25. S.R. Raghavan, H. Edlund, E.W. Kaler, Langmuir **18**, 1056 (2002).
26. C. Oelschlaeger, M. Schopferer, F. Scheffold, N. Willenbacher, Langmuir **25**, 716 (2008).
27. H. Yin, S. Lei, S. Zhu, J. Huang, J. Ye, Chem. Eur. J. **12**, 2825 (2006).
28. P.A. Hassan, J. Narayanan, C. Manohar, Curr. Sci. **80**, 980 (2001).
29. R. Granek, M.E. Cates, J. Chem. Phys. **96**, 4758 (1992).
30. M.E. Cates, Macromolecules **20**, 2289 (1987).

31. D.P. Acharya, H. Kunieda, Adv. Colloid Interface Sci. **123-126**, 401 (2006).
32. D. Varade, T. Joshi, V.K. Aswal, P.S. Goyal, P.A. Hassan, P. Bahadur, Colloids Surf. A **259**, 95 (2005).
33. H. Afifi, G. Karlsson, R.K. Heenan, C.A. Dreiss, J. Colloid Interface Sci. **378**, 125 (2012).
34. Y. Lin, Y. Qiao, X. Cheng, Y. Yan, Z. Li, J. Huang, J. Colloid Interface Sci. **369**, 238 (2012).
35. J.N. Israelachvili, *Intermolecular and Surface Forces*, second edition (Academic Press, New York, 1992).
36. Y. Talmon, *Giant Micelles – Properties and Applications* (CRC press, Boca Raton, FL, 2007).
37. T. Shikata, H. Hirata, T. Kotaka, Langmuir **4**, 354 (1988).
38. T. Shikata, M. Shiokawa, S. Imai, J. Colloid Interface Sci. **259**, 367 (2003).
39. D.R. Lide, *CRC Handbook of Chemistry and Physics* (Internet Version `http://www.hbcpnetbase.com`, CRC Press, Boca Raton, FL, 2005).
40. H. Rehage, H. Hoffmann, J. Phys. Chem. **92**, 4712 (1988).
41. B.K. Roy, S.P. Moulik, Curr. Sci. **85**, 1148 (2003).
42. I. Johnson, G. Olofsson, J. Colloid Interface Sci. **106**, 222 (1984).